

# Accurate stresses in laminated piezoelectric finite length cylinders subjected to electro-thermo-mechanical loadings

P. Desai\* and T. Kant

Department of Civil Engineering, Indian Institute of Technology Bombay, Powai, Mumbai 400 076, India

**A mixed semi-analytical computational model is presented which accounts for the coupled electrical, mechanical and thermal response of layered piezoelectric finitely long hollow circular cylinders. Boundary value problem (BVP) of an axisymmetric cylinder is considered here as a two-dimensional plane strain problem in the  $(r, z)$  plane, which is based on the exact theory of elasticity. After assuming diaphragm-supported end conditions in the longitudinal ( $z$ ) direction, the resulting mathematical model is cast in the form of first-order simultaneous ordinary differential equations which are integrated through an effective numerical integration technique by first transforming the BVP into a set of initial value problems. New results of finite length cylinders are generated and presented for future reference.**

**Keywords:** Cylinders, layered materials, piezothermo-elasticity, semi-analytical methods.

THE basic shape of piezoelectric devices is a circular cylinder which is used as a transducer, that can reflect and receive waves from the media when it is pressurized. Also, it converts the electrical pulses to mechanical energy and vice versa when pressurized. This basic device has many other useful applications like in ultrasound and ground-penetrating radar. It is important to understand the behaviour of such devices before they are used for engineering design. In view of this, the present study is focused on such cylinders which are made up of piezoelectric materials and which have several layers in thickness direction of the cylinder and polarized in radial direction. In real life such a device is made of different piezoelectric layered materials, which are subjected to electrical, mechanical and thermal loads. It is also important that such materials are orthotropic; the orthotropic phenomenon will provide particle charging and polarizing in different directions. Such a cylinder is then studied under thermal, electrical and mechanical loads. In this article, the following piezoelectric materials are used: cadmium selenide, CaSe; barium titanate,  $\text{BaTiO}_3$  (a permanently polarized material) and lead zirconate titan-

ate, PZT-5A (refs 1, 2). In addition, these materials will produce an electric field when they change dimensions as a result of an imposed mechanical force. Before these devices are used in engineering design, it is important that they are analysed accurately. Hence the present study focuses on the analysis of piezoelectric devices using an approach which is free from approximations. The uniqueness of this approach is that it requires algebraic manipulation of basic elasticity equations like equilibrium, strain displacement and constitute equations. After this manipulation, the mathematical model is presented as a two-point boundary value problem (BVP) which governs the behaviour of 2D plane strain finite length cylinder in the  $(r, z)$  plane and is governed by six first-order simultaneous partial differential equations (PDEs). These PDEs are transformed into a system of coupled first-order ordinary differential equations (ODEs) for elastostatic problem; the behaviour of a cylinder is mathematically formulated as a two-point BVP governed by a set of linear first-order ODEs. This can be written mathematically by the following equation<sup>3,4</sup>.

$$\frac{d}{dr} y(r) = A(r)y(r) + p(r). \quad (1)$$

In the domain  $r_1 \leq r \leq r_2$ , where  $y(r)$  is an  $n$ -dimensional vector of dependent variables; dependent variables in the present case can be described as  $y = (u, w, \phi, \sigma_r, \tau_{rz}, D_r)^t$ . Choice of dependent variables is important. The variables which naturally appear on  $r = \text{constant}$  are chosen as dependent variables; such variables are called intrinsic variables. The remaining variables are described as auxiliary dependent variables which are dependent on intrinsic dependent variables.  $A(r)$  is a coefficient matrix of ODEs.  $p(r)$  is an  $n$ -dimensional vector of non-homogeneous (loading) terms. For boundary conditions, any  $n/2$  elements of  $y(r)$  are specified at the two termini edges; mixed type of boundary conditions can be specified in this formulation. Recently, Desai and Kant<sup>5</sup> have obtained accurate stresses in thermoelastic laminated finite length cylinders subjected to uniformly distributed and sinusoidal loads using the above technique.

Some of the recent literature relevant for this study is described as follows. Heyliger and Pan<sup>6</sup> obtained

\*For correspondence. (e-mail: payaldesai79@gmail.com)

approximate solutions to the weak form of the governing equations of equilibrium/motion; charge and magnetic flux for laminates containing layers of potentially magneto-electroelastic material, in which there can exist elastic displacement fields, the electric potential (or voltage), and the magnetic potential. The through-thickness elastic, electric and magnetic fields of laminates composed of elastic, piezoelectric and magnetostrictive layers are considered under static condition to determine their fundamental behaviour and to study the limits of simplified plate theory in which the fields are assumed to possess a specific type of behaviour. Kapuria *et al.*<sup>7</sup> presented an exact axisymmetric piezothermoelastic solution for a simply-supported hybrid cylindrical shell made of cross-ply composite laminate with piezoelectric layers. Numerical results for hybrid shells are presented for sinusoidal and central band thermal and electrical loads. Heyliger<sup>8</sup> gave an exact three-dimensional solution of the equations of linear piezoelectricity for the static response of a finite length laminated piezoelectric cylinder with its ends simply supported. Galic and Horgan<sup>9</sup> obtained analytical solution for the axisymmetric problem of an infinitely long, radially polarized, radially orthotropic piezoelectric hollow circular cylinder. Rajapakse *et al.*<sup>10</sup> presented a theoretical study of a piezoelectric annular finite cylinder under axisymmetric loading. Ding *et al.*<sup>11</sup> obtained analytical solutions to various piezoelectric problems such as circular plate, cylinder, cone, hollow cone and annular plate. Wang and Zhong<sup>12</sup> analytically studied the problem of a finitely long circular cylindrical two layered shell of cylindrically orthotropic piezoelectric/piezomagnetic composite under pressure loading and a uniform temperature change. The analytical solution is obtained through the power series and the Fourier series expansion methods. Lim and Lau<sup>13</sup> studied the electro-mechanical behaviour of a thick, laminated actuator with piezoelectric and isotropic laminae under externally applied electric loading using a new two-dimensional computational model. The model was analysed using Timoshenko thick beam theory. Wu and Tsai<sup>14</sup> have recently presented the three-dimensional coupled analysis of simply-supported functionally graded (FG) and piezoelectric sandwich cylinders under electro-mechanical loads using modified Pagano method. The modifications in the original Pagano method were replacement of displacement-based formulation with mixed formulation and a set of complex-valued solutions of system equation was transferred to a corresponding set of real-valued solutions. A transfer matrix method is used to analyse the effect of layers. Ying *et al.*<sup>15</sup> proposed a stochastic response analysis method for piezoelectric thick axisymmetric hollow cylinders subjected to boundary stochastic excitations based on the transformations of electric potentials and displacements, the Galerkin method and the theory of random vibration. The authors have claimed that the proposed analysis method is applicable to hollow

cylinders with arbitrary thickness under various non-white stochastic excitations of inner and/or outer pressures and electric potentials. Larbi and Deu<sup>16</sup> presented a three-dimensional exact mixed state-space solution for the free-vibration analysis of simply-supported arbitrarily thick laminated piezoceramic hollow cylinders completely filled with fluid. Saviz and Mohammadpourfard<sup>17</sup> presented dynamic analysis for simply-supported laminated cylindrical shell with orthotropic layers bounded with piezoelectric layers and subjected to local ring/pinch loads. The piezoelectric layers serve as sensors/actuators. The governing elasticity equations are reduced to ODEs by means of trigonometric function expansion. The resulting equations are solved by Galerkin's finite element method in radial direction. Li *et al.*<sup>18</sup> analysed an axisymmetric electroelastic problem of hollow radially polarized piezoceramic cylinders made of FG materials. For the material properties with power-law profile, a closed-form solution is obtained. For a general gradient variation, an analytic approach is suggested, which reduces the problem to a Fredholm integral equation. Khdeir and Aldraihem<sup>19</sup> formulated and developed models and analytical solutions for the static behaviour of cross-ply smart laminated shells with piezoelectric laminae. The models are based on a rigorous first-order shell theory. The state-space approach is used to find exact solutions for the static response of cross-ply spherical, cylindrical and doubly curved shells with various boundary conditions. It was noted here that the past literature covers the use of state-space approach for layered media, in which use has been made of the continuity conditions at each interface between any two adjacent sub-layers. Also, it is seen from the literature that accurate benchmark solutions using exact elasticity theory are rare for finite length cylinders under thermo-mechanical-electro loadings.

## Formulation of the problem

The basic governing equations which describe the behaviour of a finite length thermo-electro-mechanical cylinder are written below.

### Equilibrium equations

Two-dimensional stress equilibrium equations for finite length cylinder in cylindrical coordinates can be written as<sup>20</sup> (Figure 1)

$$\sigma_{r,r} + \tau_{rz,z} + \frac{\sigma_r - \sigma_\theta}{r} = 0, \quad \tau_{rz,r} + \sigma_{z,r} + \frac{\tau_{rz}}{r} = 0. \quad (2)$$

For piezoelectric cylinder additional electrostatic charge equilibrium equation<sup>2</sup> is written as

$$D_{r,r} + D_{z,z} + \frac{D_r}{r} = 0. \quad (3)$$

*Strain-displacement relations*

Two-dimensional strain-displacement relations in cylindrical coordinates are

$$\varepsilon_r = u_{,r}; \quad \varepsilon_\theta = \frac{u}{r}; \quad \varepsilon_z = w_{,z}; \quad \varepsilon_{rz} = u_{,z} + w_{,r}.$$

Electric potential  $\phi$  is defined by the following relations

$$E_r = -\phi_{,r}; \quad E_z = -\phi_{,z}. \quad (4)$$

*Stress-displacement relations*

Stresses in terms of displacement components for cylindrically orthotropic piezoelectric material can be cast as follows<sup>1,2</sup>

$$\begin{aligned} \sigma_r &= C_{11}u_{,r} + C_{12}\frac{u}{r} + C_{13}w_{,z} + e_{11}\phi_{,r} - \beta_1 T, \\ \sigma_\theta &= C_{21}u_{,r} + C_{22}\frac{u}{r} + C_{23}w_{,z} + e_{12}\phi_{,r} - \beta_2 T, \\ \sigma_z &= C_{31}u_{,r} + C_{32}\frac{u}{r} + C_{33}w_{,z} + e_{13}\phi_{,r} - \beta_3 T, \\ \tau_{rz} &= G(w_{,r} + u_{,z}) + e_{15}\phi_{,z}. \end{aligned} \quad (5)$$

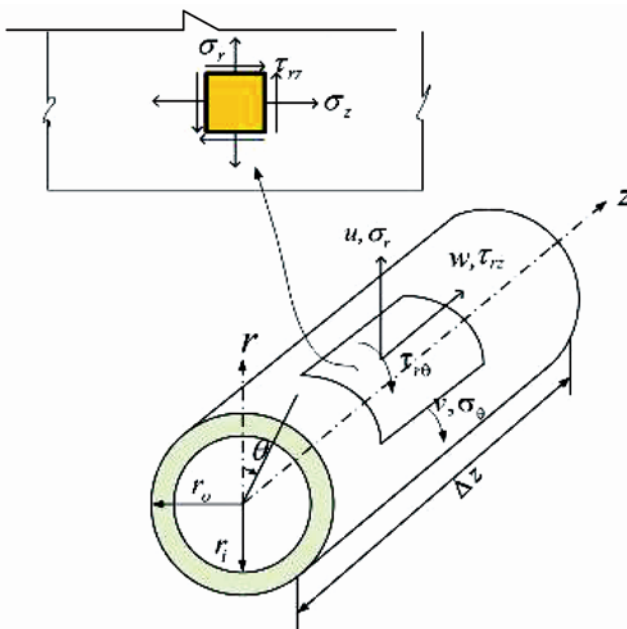


**Figure 1.** Cylindrical coordinates and fundamental dependent variables in a cylinder.

Constitutive relations for the electric field are defined as follows

$$D_r = e_{11}u_{,r} + e_{12}\frac{u}{r} + e_{13}w_{,z} - \varepsilon_{11}\phi_{,r} + q_1 T,$$

$$D_z = e_{15}\varepsilon_{rz} - \varepsilon_{33},$$

$$E_z = e_{15}(w_{,r} + u_{,z}) - \varepsilon_{33}\phi_{,z}.$$

In the above, the parameters have the following definitions.  $u$  is the radial displacement and  $\phi = \phi(r)$  is the electric potential. The elastic constants are  $C_{11}$ ,  $C_{12}$ ,  $C_{22}$ ,  $C_{23}$ ,  $C_{31}$  and  $C_{33}$ . The piezoelectric constants are  $e_{11}$ ,  $e_{12}$ ,  $e_{13}$ ,  $e_{15}$  and  $\varepsilon_{11}$ ,  $\varepsilon_{33}$  are the dielectric permittivities at constant strain. Here  $\beta_1$ ,  $\beta_2$ ,  $\beta_3$  and  $q_1$  are stress-temperature coefficients.

*Boundary conditions*

Boundary conditions in the longitudinal and radial directions for elastic and electric fields are defined as follows

$$\text{At } z = 0, l, \quad u = \sigma_z = D_z = 0;$$

$$\text{At } r = r_i, \quad \sigma_r = \tau_{rz} = \phi = 0,$$

$$\text{At } r = r_0, \quad \sigma_r = \tau_{rz} = \phi = 0, \quad (6)$$

where  $l$  is the length,  $r_i$  the inner radius and  $r_0$  the outer radius of a hollow cylinder. Load  $T(r, z)$  can be represented in terms of Fourier series in general form as follows

$$T(r, z) = \sum_{m=1,3,5..}^N T_m(r) \sin \frac{m\pi z}{l}, \quad (7)$$

where  $T_m$  is the Fourier load coefficient which can be determined using the orthogonality conditions, and for sinusoidal loading,  $T(r, z) = T_0(r) \sin(m\pi z/l)$ ,  $T_0$  is the maximum intensity of temperature at  $z = l/2$ .

*First-order partial differential equations*

Radial direction  $r$  is chosen as the preferred independent coordinate. Six fundamental dependent variables, viz. displacements,  $u$  and  $w$ , electric potential  $\phi$  and the corresponding stresses,  $\sigma_r$ ,  $\tau_{rz}$  and  $D_r$  that occur naturally on a tangent plane  $r = \text{constant}$ , are chosen in the radial direction. Circumferential stress  $\sigma_\theta$ , axial stress  $\sigma_z$  and axial electric displacement  $D_z$  are treated here as auxiliary variables since these are found to be dependent on the chosen fundamental variables. A set of six first-order PDEs in independent coordinate  $r$  which involves only

fundamental variables is obtained through algebraic manipulation of eqs (2)–(5). These are

$$\frac{\partial}{\partial r} \begin{pmatrix} u \\ w \\ \phi \\ \sigma_r \\ \tau_{rz} \\ D_r \end{pmatrix} = \begin{pmatrix} A_{11} & A_{12} & 0 & A_{14} & 0 & A_{16} \\ A_{21} & 0 & A_{23} & 0 & A_{25} & 0 \\ A_{31} & A_{32} & 0 & A_{34} & 0 & A_{36} \\ A_{41} & A_{42} & 0 & A_{44} & A_{45} & A_{46} \\ A_{51} & A_{52} & 0 & A_{54} & A_{55} & A_{56} \\ A_{61} & 0 & A_{63} & 0 & A_{65} & A_{66} \end{pmatrix} \begin{pmatrix} u \\ w \\ \phi \\ \sigma_r \\ \tau_{rz} \\ D_r \end{pmatrix} + T \begin{pmatrix} d_{11} \\ d_{21} \\ d_{31} \\ d_{41} \\ d_{51} \\ d_{61} \end{pmatrix}. \quad (8)$$

$A$  and  $d$  are the coefficient matrices described in Appendix 1.

### Basic fundamental variables

Variations of the six fundamental dependent variables which completely satisfy the boundary conditions of simple (diaphragm) supports at  $z = 0, l$  can then be assumed as

$$\begin{aligned} \sigma_r(r, z) &= \sigma^i(r) \sin \frac{\pi z}{l}; & \tau_{rz}(r, z) &= \tau^i(r) \cos \frac{\pi z}{l}; \\ u(r, z) &= U^i(r) \sin \frac{\pi z}{l}; & w(r, z) &= W^i(r) \cos \frac{\pi z}{l}; \\ D_r(r, z) &= D^i(r) \sin \frac{\pi z}{l}; & \phi(r, z) &= \Phi^i(r) \sin \frac{\pi z}{l}. \end{aligned} \quad (9)$$

### First-order ordinary differential equations

Substitution of fundamental variables given in eq. (9) into eq. (8) and simplification resulting from orthogonality conditions of trigonometric functions lead to the following first-order simultaneous ODEs involving amplitudes of mixed set of fundamental variables as given below

$$\begin{aligned} \frac{d}{dr} \begin{pmatrix} U^i(r) \\ W^i(r) \\ \Phi^i(r) \\ \sigma^i(r) \\ \tau^i(r) \\ D^i(r) \end{pmatrix} &= \begin{pmatrix} B_{11} & B_{12} & 0 & B_{14} & 0 & B_{16} \\ B_{21} & 0 & B_{23} & 0 & B_{25} & 0 \\ B_{31} & B_{32} & 0 & B_{34} & 0 & B_{36} \\ B_{41} & B_{42} & 0 & B_{44} & B_{45} & B_{46} \\ B_{51} & B_{52} & 0 & B_{54} & B_{55} & B_{56} \\ B_{61} & 0 & B_{63} & 0 & B_{65} & B_{66} \end{pmatrix} \begin{pmatrix} U^i(r) \\ W^i(r) \\ \Phi^i(r) \\ \sigma^i(r) \\ \tau^i(r) \\ D^i(r) \end{pmatrix} \\ &\times \begin{pmatrix} U^i(r) \\ W^i(r) \\ \Phi^i(r) \\ \sigma^i(r) \\ \tau^i(r) \\ D^i(r) \end{pmatrix} + T(r) \begin{pmatrix} f_{11} \\ f_{21} \\ f_{31} \\ f_{41} \\ f_{51} \\ f_{61} \end{pmatrix} \end{aligned} \quad (10)$$

$B$  and  $f$  are the coefficient matrices described in Appendix 2.

The above system of first-order simultaneous ODEs (eq. (10)) together with the appropriate boundary conditions at the inner and outer edges of the cylinder (eq. (6)) form a two-point BVP. However, a BVP in ODEs cannot be numerically integrated as only half of the dependent variables (three) are known at the initial edge and numerical integration of an ODE is intrinsically an initial value problem (IVP). It becomes necessary to transform the problem into a set of IVPs. The initial values of the remaining three fundamental variables must be selected so that the complete solution satisfies the three specified conditions at the terminal boundary. The  $n$ th ( $n = 6$  here)-order BVP is transformed into a set of  $(n/2 + 1)$  IVPs. ODEs are integrated from the initial edge to the final edge using the initial values as shown in Table 1. The  $n/2 + 1$  solutions given in Table 1 may be thought of as: (i) one non-homogeneous integration which includes all the non-homogeneous terms (e.g. loading) and the known  $n/2$  quantities at the starting edge, with the unknown  $n/2$  quantities at the starting edge set as zero; (ii)  $n/2$  homogeneous integrations which are carried out by setting the known quantities at the starting edge as zero and choosing the  $n/2$  unknown quantities at the starting edge as unit values in succession and deleting the non-homogeneous terms from the ODEs. The solutions at the terminal boundary corresponding to the initial values are given in the right side columns in Table 1. A linear combination of the  $(n/2 + 1)$  solutions must satisfy the boundary conditions at the terminal edge, i.e.

$$\begin{pmatrix} Y_{3,0} \\ Y_{4,0} \\ Y_{5,0} \end{pmatrix} + \begin{pmatrix} Y_{3,1} & Y_{3,2} & Y_{3,3} \\ Y_{4,1} & Y_{4,2} & Y_{4,3} \\ Y_{5,1} & Y_{5,2} & Y_{5,3} \end{pmatrix} \begin{pmatrix} X_1 \\ X_2 \\ X_3 \end{pmatrix} = \begin{pmatrix} \bar{Y}_3 \\ \bar{Y}_4 \\ \bar{Y}_5 \end{pmatrix}$$

or

$$Y_{i,0} + Y_{i,j} X_j = \bar{Y}_i \quad \text{or} \quad X_j = [Y_{i,j}]^{-1} (\bar{Y}_i - Y_{i,0}), \quad (11)$$

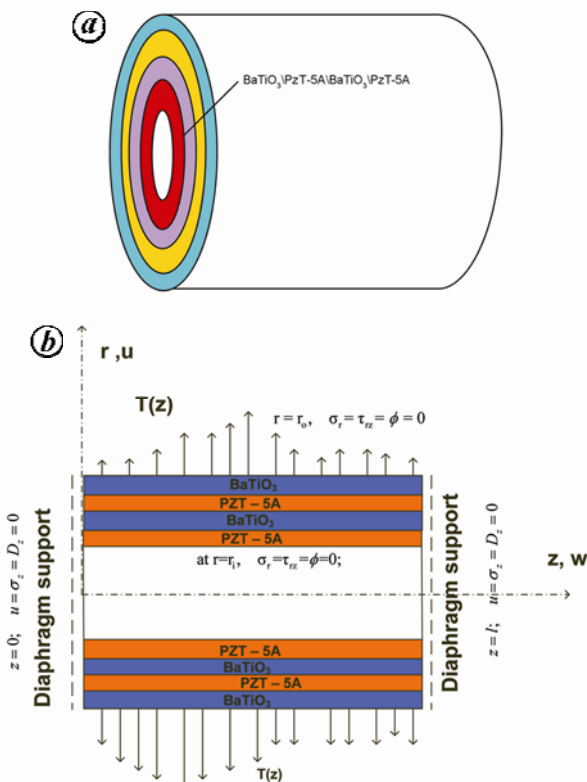
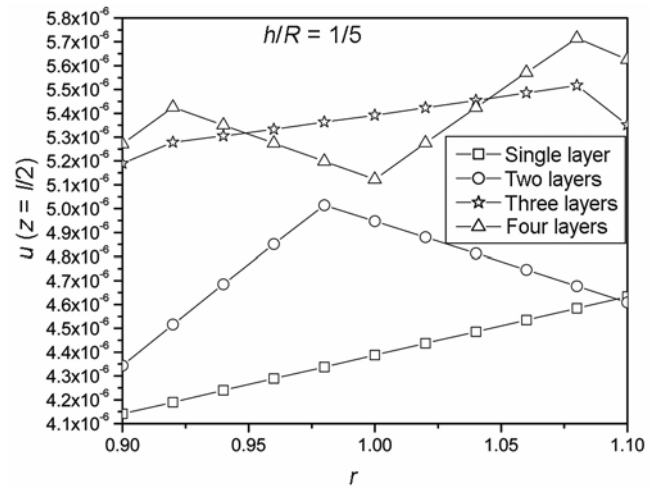
where  $i$  indicates the  $n/2$  variables consistent with the specified boundary values at the terminal edge,  $j$  refers to solution number and ranges from 1 to  $n/2$ ,  $\bar{Y}_i$  is a vector of specified dependent variables at the terminal boundary and  $X_j$  is a vector of unknown dependent variables at the starting edge. Finally, a non-homogeneous integration with all the dependent variables known at the starting edge is carried out to get the desired results. Fourth-order Runge–Kutta algorithm with modifications suggested by Gill<sup>21</sup> has been used for the numerical integration of the IVPs. Stability of the present numerical technique is checked via convergence study by taking different step sizes in the Runge–Kutta–Gill algorithm.

**Table 1.** Conversion of boundary value problem into initial value problems

Integration number	Initial boundary						Terminal boundary						Load term
	$u$	$w$	$\phi$	$\sigma_r$	$\tau_{rz}$	$D_r$	$u$	$w$	$\phi$	$\sigma_r$	$\tau_{rz}$	$D_r$	
0	0	0	(Specified)	(Specified)	(Specified)	0	$Y_{1,0}$	$Y_{2,0}$	$Y_{3,0}$	$Y_{4,0}$	$Y_{5,0}$	$Y_{6,0}$	Include
1	1	0	0	0	0	0	$Y_{1,1}$	$Y_{2,1}$	$Y_{3,1}$	$Y_{4,1}$	$Y_{5,1}$	$Y_{6,1}$	Delete
2	0	1	0	0	0	0	$Y_{1,2}$	$Y_{2,2}$	$Y_{3,2}$	$Y_{4,2}$	$Y_{5,2}$	$Y_{6,2}$	Delete
3	0	0	0	0	0	1	$Y_{1,3}$	$Y_{2,3}$	$Y_{3,3}$	$Y_{4,3}$	$Y_{5,3}$	$Y_{6,3}$	Delete
Final integration	$X_1$	$X_2$	(Specified)	(Specified)	(Specified)	$X_3$	Correct value $X_1$	Correct value $X_2$	Known	Known	Known	Correct value $X_3$	Include

**Table 2.** Piezoelectric material property

PZT-5A	CaSe	BaTiO <sub>3</sub>
$C_{33} = 99.201 \times 10^9$	$C_{33} = 74.1 \times 10^9$	$C_{33} = 150.0 \times 10^9$
$C_{22} = 99.201 \times 10^9$	$C_{22} = 74.1 \times 10^9$	$C_{22} = 150.0 \times 10^9$
$C_{11} = 86.856 \times 10^9$	$C_{11} = 83.6 \times 10^9$	$C_{11} = 146.0 \times 10^9$
$C_{32} = 54.016 \times 10^9$	$C_{32} = 45.2 \times 10^9$	$C_{32} = 66.0 \times 10^9$
$C_{12} = 50.778 \times 10^9$	$C_{12} = 39.3 \times 10^9$	$C_{12} = 66.0 \times 10^9$
$C_{13} = 50.778 \times 10^9$	$C_{13} = 39.3 \times 10^9$	$C_{13} = 66.0 \times 10^9$
$G_{rz} = 21.100 \times 10^9$	$G_{rz} = 13.17 \times 10^9$	$G_{rz} = 44 \times 10^9$
$\alpha_3 = 3.314 \times 10^5 \text{ Pa K}^{-1}$	$\alpha_3 = 0.621 \times 10^6 \text{ Pa K}^{-1}$	$\alpha_3 = 1.92 \times 10^6 \text{ Pa K}^{-1}$
$\alpha_2 = 3.314 \times 10^5 \text{ Pa K}^{-1}$	$\alpha_2 = 0.621 \times 10^6 \text{ Pa K}^{-1}$	$\alpha_2 = 1.92 \times 10^6 \text{ Pa K}^{-1}$
$\alpha_1 = 3.260 \times 10^5 \text{ Pa K}^{-1}$	$\alpha_1 = 0.551 \times 10^6 \text{ Pa K}^{-1}$	$\alpha_1 = 1.65 \times 10^6 \text{ Pa K}^{-1}$
$e_{15} = 12.322$	$e_{15} = -0.138 \text{ C/m}^2$	$e_{15} = 11.4 \text{ C/m}^2$
$e_{13} = -7.209$	$e_{13} = -0.160$	$e_{13} = -4.35$
$e_{12} = -7.209$	$e_{12} = -0.160$	$e_{12} = -4.35$
$e_{11} = 15.118$	$e_{11} = 0.347$	$e_{11} = 17.5$
$\epsilon_{11} = 150 \times 10^{-10} \text{ F/m}$	$\epsilon_{11} = 90.2 \times 10^{-12} \text{ F/m}$	$\epsilon_{11} = 15.04 \times 10^{-9} \text{ F/m}$
$q_1 = 700 \times 10^{-6} \text{ C/m}^2 \text{K}$	$q_1 = -2.94 \times 10^{-6} \text{ C/m}^2 \text{K}$	$q_1 = 213.5 \times 10^{-6} \text{ C/m}^2 \text{K}$

**Figure 2.** *a*, Number of piezoelectric material layers in thick orthotropic cylinder. *b*, Diaphragm supported cylinder.**Figure 3.** Variation of radial displacement with thickness for single and multilayer piezoelectric thick cylinders.

### Numerical example

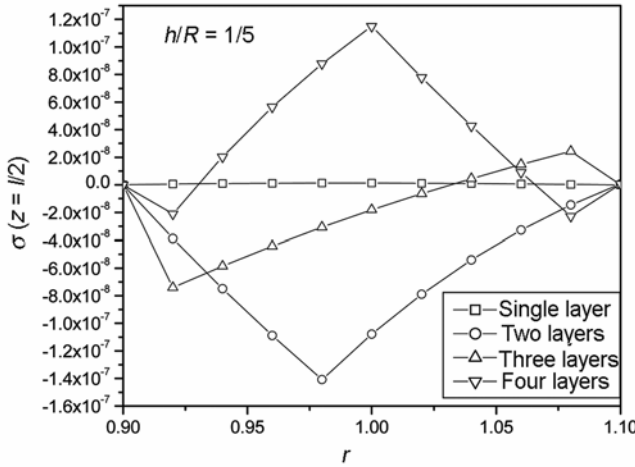
In the present work, a piezoelectric cylinder of single layer-CaSe and combinations of piezoelectric layers BaTiO<sub>3</sub>/PZT-5A (two layers), BaTiO<sub>3</sub>/CaSe/PZT-5A (three layers) and BaTiO<sub>3</sub>/PZT-5A/BaTiO<sub>3</sub>/PZT-5A (four layers) have been studied (Figure 2). Piezoelectric and pyroelectric material properties are taken from Wang

**Table 3.** Comparison of non dimensionalized results (value/10<sup>6</sup>) of present finite length cylinder with long cylinder for three layers

$r$	$u$ – Long cylinder	$u$ – Short cylinder	$\Phi$ – Long cylinder	$\Phi$ – Short cylinder	$\sigma$ – Long cylinder	$\sigma$ – Short cylinder
0.9	52.1700	51.9000	0.0000	0.0000	0.0000	0.0000
0.92	53.0400	52.7800	0.3899	0.3926	-0.7280	-0.7404
0.94	53.3000	53.0500	0.2880	0.3062	-0.5710	-0.5850
0.96	53.5700	53.3300	0.1723	0.2017	-0.4258	-0.4405
0.98	53.8600	53.6300	0.0428	0.0792	-0.2914	-0.3060
1	54.1500	53.9200	-0.1002	-0.0613	-0.1667	-0.1807
1.02	54.4600	54.2300	-0.2566	-0.2196	-0.0511	-0.0638
1.04	54.7700	54.5400	-0.4262	-0.3956	0.0562	0.0454
1.06	55.1000	54.8500	-0.6088	-0.5894	0.1559	0.1475
1.08	55.4300	55.1700	-0.8043	-0.8009	0.2486	0.2429
1.1	53.7800	53.5100	0.0000	0.0000	0.0000	0.0000

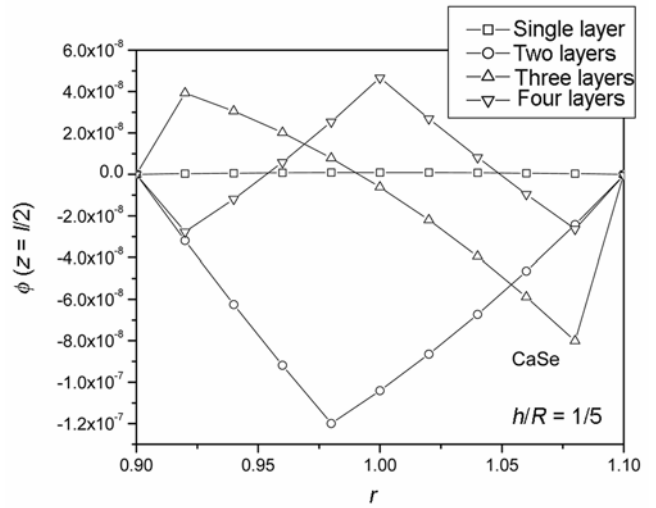
**Table 4.** Maximum value (value/10<sup>6</sup>) of fundamental quantities through thickness

	$u$	$w$	$\Phi$	$\sigma_r$	$\tau_{rz}$	$D_r$
Thick						
1 layer	46.3300	-59.4000	0.0093	0.0130	0.0524	243.9000
2 layer	50.1400	-64.5300	-1.2000	-1.4090	1.1790	-1189.0000
3 layer	55.1700	-73.1100	0.0792	-0.7404	0.5872	9.0270
4 layer	56.2500	-72.8800	0.4665	1.1510	-0.7764	-1106.0000
Thin						
1 layer	44.2000	-56.3400	0.0001	0.0001	0.0005	220.8000
2 layer	48.2300	-61.5600	-0.0875	-0.1582	0.1250	-1106.0000
3 layer	54.3400	-69.5200	-0.0798	-0.0725	0.0570	8.3490
4 layer	54.2500	-69.0900	0.0612	0.0948	-0.0731	-998.3000

**Figure 4.** Variation of normal radial stress with thickness for single and multilayer piezoelectric thick cylinders.

and Zhong<sup>12</sup>, which are shown in Table 2. Two  $h/R$  ratios which cover thick and thin cylinders were studied. Uniform temperature distribution through thickness has been considered. Here,  $T_1(r)$  is taken as unity for simplicity. The following non-dimensional parameters were used.

$$\bar{\sigma}_r = \frac{\sigma_r}{C_{11}}, \quad \bar{\phi} = \frac{e_{11}}{C_{11}} \frac{\phi}{r_i}, \quad \bar{D}_r = \frac{D_r}{e_{12}}, \quad \bar{u} = \frac{u}{r_i},$$

**Figure 5.** Variation of electrical potential with thickness for single and multilayer piezoelectric thick cylinders.

$$\bar{w} = \frac{w}{r_i}, \quad \bar{\tau}_{rz} = \frac{\tau_{rz}}{C_{11}} a. \quad (12)$$

Shear stresses, radial normal stresses, electric potential and radial electric displacements were obtained as a part of the numerical analysis in the present work. It is seen that piezoelectric material properties have significant

effect on the stresses and displacements of finite length cylinders. Figures 3–5 show the important quantities such as radial displacement, radial stress and electric potential

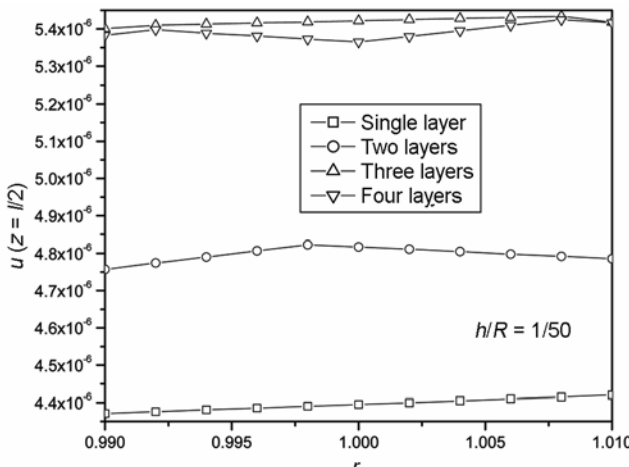


Figure 6. Variation of radial displacement with thickness for single and multilayer piezoelectric thin cylinders.

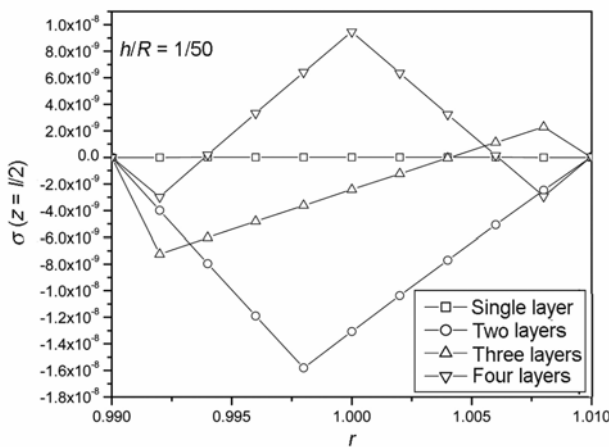


Figure 7. Variation of radial stress with thickness for single and multilayer piezoelectric thin cylinders.

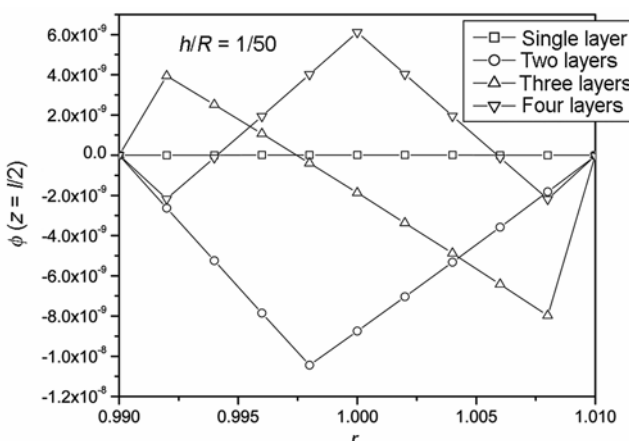


Figure 8. Variation of electrical potential with thickness for single and multilayer piezoelectric thin cylinders.

for all layers of piezoelectric cylinder for  $h/R$  ratio as 1/5. Figures 6–8 show the radial displacement, radial stress and electric potential for all layers of piezoelectric cylinder for  $h/R$  ratio 1/50. From these figures, it is seen that higher values of radial stress and electric potential develop at the inner points of the cylinder thickness. Figures 9–11 show the comparison of results for infinitely long cylinder and finite length cylinder for validation purpose. Derivations for infinitely long cylinders are given in Appendix 3 for reference purpose. Good agreement is seen in Figures 9–11 between the two formulations. Table 3 presents the numerical values of such a comparison. Table 4 shows the maximum values of all the basic fundamental variables. Radial stress is zero at the top and bottom surfaces of the thickness of the cylinder as expected, because of applied zero normal stress at the top and bottom surfaces as boundary conditions.

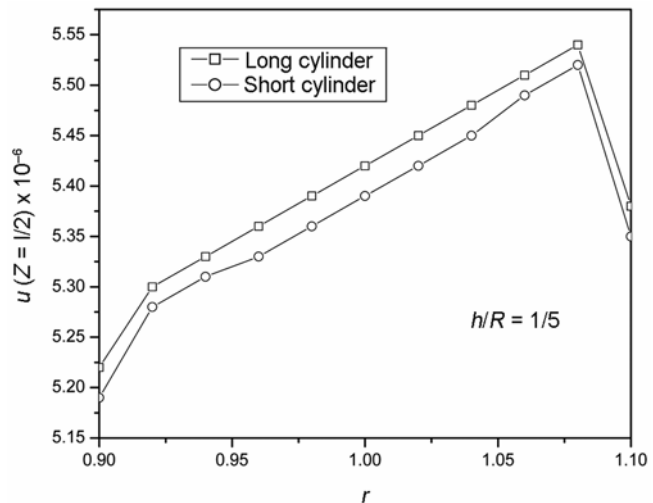


Figure 9. Comparison of radial displacement with thickness for three-layer piezoelectric long and short, thick cylinders.

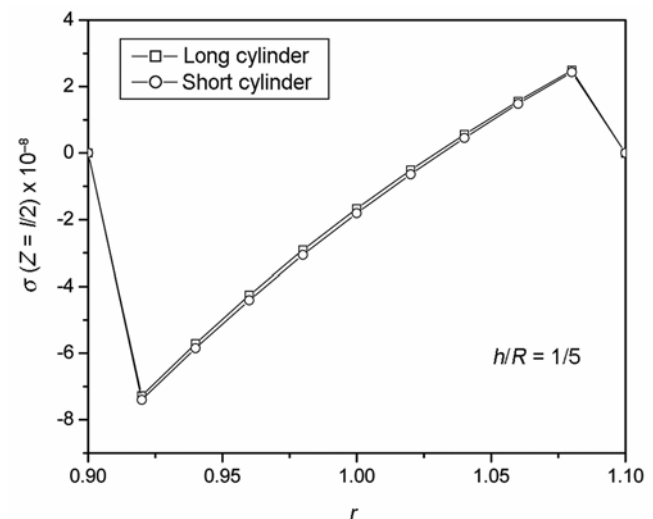
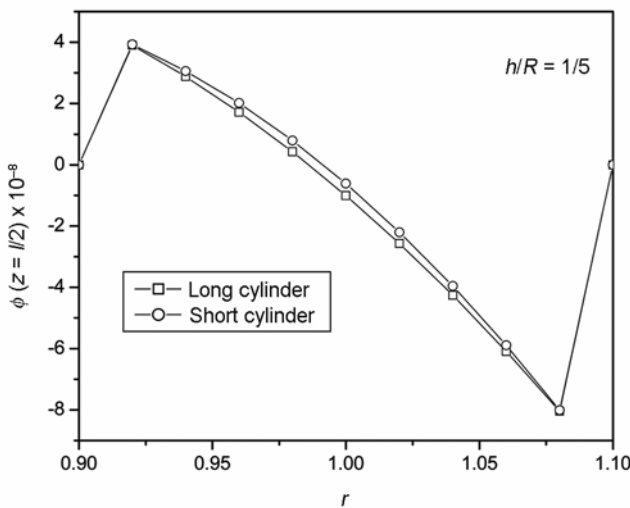


Figure 10. Comparison of radial stress with thickness for three layer-piezoelectric long and short, thick cylinders.



**Figure 11.** Comparison of electric potential with thickness for three-layer piezoelectric long and short, thick cylinders.

Similar behaviour is seen for the electric potential. Even if zero electric potential is applied at top and bottom surfaces, the cylinder develops some potential values through its thickness. This is because of piezoelectric effect considered in the material. Thus, the piezoelectric cylinder acts as a sensor. For  $h/R$  ratio equal to 1/5, radial stress variation in each layer is seen to be slightly non-linear. Whereas linear variation is seen in case of ( $h/R = 1/50$ ) thin cylinders.

## Conclusion

An attempt has been made here to analyse the piezoelectric device which is subjected to electric field in addition to elastostatic and temperature fields through exact semi-analytical cum numerical approach, which differs from conventional approximate finite element approach and is also free from any assumptions in the theory. The model is based on the solutions of a two-point BVP governed by ODEs through thickness of the cylinder. Fourth-order Runge–Kutta–Gill algorithm was used for numerical integration. The results are useful when one is designing pressurized cylinders made up of different layers of piezoelectric materials which are used as transducers and other sensing devices. This approach can be applied with ease to thick, multilayer cylinders. The technique is convenient to obtain the interlaminar stresses in a natural way, since the continuity conditions of transverse interlaminar stresses and displacements between the layers (lamine interfaces) are satisfied automatically via the numerical integration. This is an important feature of the proposed model. Also, it involves mixed variables in the derivations, both stresses and displacements are obtained accurately simultaneously. Numerical results

presented for different  $h/R$  ratios will be useful for future reference and should serve as benchmark results.

## Appendix 1.

$$A_{11} = \frac{1}{r} \left( \frac{e_{11}c_{12}e_{11}}{c_{11}\epsilon_{11}c_{11}} a - \frac{c_{12}}{c_{11}} - \frac{e_{11}e_{12}}{c_{11}\epsilon_{11}} a \right),$$

$$A_{12} = \frac{\partial \{ \}}{\partial z} \left( \frac{e_{11}e_{11}}{c_{11}\epsilon_{11}} a \frac{c_{13}}{c_{11}} - \frac{e_{11}e_{13}}{c_{11}\epsilon_{11}} a - \frac{c_{13}}{c_{11}} \right),$$

$$A_{14} = \left( \frac{1}{c_{11}} - \frac{e_{11}e_{11}}{c_{11}\epsilon_{11}} \frac{a}{c_{11}} \right), \quad A_{16} = \frac{e_{11}a}{c_{11}\epsilon_{11}},$$

$$A_{21} = -\frac{\partial}{\partial z}, \quad A_{23} = -\frac{e_{15}}{G} \frac{\partial \{ \}}{\partial z}, \quad A_{25} = \frac{1}{G},$$

$$A_{31} = \frac{1}{r} \left( \frac{e_{12}}{\epsilon_{11}} a - \frac{c_{12}e_{11}}{\epsilon_{11}c_{11}} a \right),$$

$$A_{32} = \left( \frac{e_{13}}{\epsilon_{11}} a - \frac{e_{11}}{\epsilon_{11}} a \frac{c_{13}}{c_{11}} \right) \frac{\partial \{ \}}{\partial z},$$

$$A_{34} = \left( \frac{e_{11}}{\epsilon_{11}c_{11}} a \right), \quad A_{36} = -\frac{1}{\epsilon_{11}} a,$$

$$A_{41} = \frac{1}{r^2} \left( \begin{array}{l} \frac{c_{21}e_{11}c_{12}e_{11}a}{c_{11}\epsilon_{11}c_{11}} - \frac{c_{21}c_{12}}{c_{11}} - \frac{e_{11}e_{12}ac_{21}}{c_{11}\epsilon_{11}} \\ + c_{22} + \frac{e_{12}e_{12}a}{\epsilon_{11}} - \frac{e_{12}c_{12}e_{11}a}{\epsilon_{11}c_{11}} \end{array} \right),$$

$$A_{42} = \frac{1}{r} \left( \begin{array}{l} \frac{c_{21}e_{11}e_{11}ac_{13}}{c_{11}\epsilon_{11}c_{11}} - \frac{c_{21}c_{13}}{c_{11}} - \frac{c_{21}e_{11}e_{13}a}{c_{11}\epsilon_{11}} \\ + c_{23} - \frac{e_{11}ac_{13}e_{12}}{\epsilon_{11}c_{11}} + \frac{e_{12}e_{13}}{\epsilon_{11}} a \end{array} \right) \frac{\partial \{ \}}{\partial z},$$

$$A_{44} = \frac{1}{r} \left( \frac{c_{21}}{c_{11}} - 1 - \frac{c_{21}e_{11}e_{11}a}{c_{11}\epsilon_{11}c_{11}} + \frac{e_{12}e_{11}a}{\epsilon_{11}c_{11}} \right),$$

$$A_{45} = -\frac{\partial \{ \}}{\partial z}, \quad A_{46} = \frac{1}{r} \left( \frac{c_{21}e_{11}a}{c_{11}\epsilon_{11}} - \frac{e_{12}a}{\epsilon_{11}} \right),$$

$$A_{51} = -\frac{\partial}{\partial z} \left\{ \frac{1}{r} \right\} \left( \begin{array}{l} \frac{e_{11}c_{12}e_{11}ac_{31}}{c_{11}\epsilon_{11}c_{11}} - \frac{c_{31}c_{12}}{c_{11}} - \frac{c_{31}e_{11}e_{12}a}{c_{11}\epsilon_{11}} \\ + c_{32} + \frac{e_{13}e_{12}}{\epsilon_{11}} a - \frac{e_{13}c_{12}e_{11}a}{\epsilon_{11}c_{11}} \end{array} \right),$$

$$A_{52} = -\frac{\partial^2}{\partial z^2} \begin{pmatrix} \frac{c_{31}e_{11}e_{11}ac_{13}}{c_{11}\epsilon_{11}c_{11}} - \frac{c_{31}e_{11}e_{13}a}{c_{11}\epsilon_{11}} - \frac{c_{31}c_{13}}{c_{11}} \\ +c_{33} - \frac{e_{13}e_{11}ac_{13}}{\epsilon_{11}c_{11}} + \frac{e_{13}e_{13}}{\epsilon_{11}}a \end{pmatrix},$$

$$A_{53} = -\frac{\partial \{ \}}{\partial z} \left( \frac{c_{31}}{c_{11}} - c_{31} \frac{e_{11}e_{11}a}{c_{11}\epsilon_{11}c_{11}} + \frac{e_{11}ae_{13}}{\epsilon_{11}c_{11}} \right),$$

$$A_{54} = -\frac{1}{r}, \quad A_{56} = -\left( \frac{c_{31}e_{11}a}{c_{11}\epsilon_{11}} - \frac{e_{13}}{\epsilon_{11}}a \right) \frac{\partial \{ \}}{\partial z},$$

$$A_{61} = \frac{\partial^2}{\partial z^2} e_{15}, \quad A_{63} = \frac{e_{15}e_{15}}{G} \frac{\partial^2}{\partial z^2} + \epsilon_{11} \frac{\partial^2}{\partial z^2},$$

$$A_{65} = -\frac{e_{15}}{G} \frac{\partial}{\partial z}, \quad A_{66} = -\frac{D_r}{r}, \quad a = \frac{1}{1 + \frac{e_{11}e_{11}}{\epsilon_{11}c_{11}}},$$

## Appendix 2.

$$B_{11} = \frac{1}{r} \left( \frac{e_{11}c_{12}e_{11}}{c_{11}\epsilon_{11}c_{11}}a - \frac{c_{12}}{c_{11}} - \frac{e_{11}e_{12}}{c_{11}\epsilon_{11}}a \right),$$

$$B_{12} = -\frac{\pi}{l} \left( \frac{e_{11}e_{11}}{c_{11}\epsilon_{11}}a \frac{c_{13}}{c_{11}} - \frac{e_{11}e_{13}}{c_{11}\epsilon_{11}}a - \frac{c_{13}}{c_{11}} \right),$$

$$B_{14} = \left( \frac{1}{c_{11}} - \frac{e_{11}e_{11}}{c_{11}\epsilon_{11}} \frac{a}{c_{11}} \right), \quad B_{16} = \frac{e_{11}a}{c_{11}\epsilon_{11}},$$

$$B_{21} = -\frac{\pi}{l}, \quad B_{23} = -\frac{e_{15}}{G} \frac{\pi}{l}, \quad B_{25} = \frac{1}{G},$$

$$B_{31} = \frac{1}{r} \left( \frac{e_{12}}{\epsilon_{11}}a - \frac{c_{12}e_{11}}{\epsilon_{11}c_{11}}a \right),$$

$$B_{32} = -\frac{\pi}{l} \left( \frac{e_{13}}{\epsilon_{11}}a - \frac{e_{11}}{\epsilon_{11}}a \frac{c_{13}}{c_{11}} \right),$$

$$B_{34} = \left( \frac{e_{11}}{\epsilon_{11}c_{11}}a \right), \quad B_{36} = -\frac{1}{\epsilon_{11}}a,$$

$$B_{41} = \frac{1}{r^2} \left( \begin{array}{c} \frac{c_{21}e_{11}c_{12}e_{11}a}{c_{11}\epsilon_{11}c_{11}} - \frac{c_{21}c_{12}}{c_{11}} - \frac{e_{11}e_{12}ac_{21}}{c_{11}\epsilon_{11}} \\ +c_{22} + \frac{e_{12}e_{12}a}{\epsilon_{11}} - \frac{e_{12}c_{12}e_{11}a}{\epsilon_{11}c_{11}} \end{array} \right),$$

$$B_{42} = -\frac{\pi}{l} \frac{1}{r} \left( \begin{array}{c} \frac{c_{21}e_{11}e_{11}ac_{13}}{c_{11}\epsilon_{11}c_{11}} - \frac{c_{21}c_{13}}{c_{11}} - \frac{c_{21}e_{11}e_{13}a}{c_{11}\epsilon_{11}} \\ +c_{23} - \frac{e_{11}ac_{13}e_{12}}{\epsilon_{11}c_{11}} + \frac{e_{12}e_{13}}{\epsilon_{11}}a \end{array} \right),$$

$$B_{44} = \frac{1}{r} \left( \frac{c_{21}}{c_{11}} - 1 - \frac{c_{21}e_{11}e_{11}a}{c_{11}\epsilon_{11}c_{11}} + \frac{e_{12}e_{11}a}{\epsilon_{11}c_{11}} \right),$$

$$B_{45} = \frac{\pi}{l}, \quad B_{46} = \frac{1}{r} \left( \frac{c_{21}e_{11}a}{c_{11}\epsilon_{11}} - \frac{e_{12}a}{\epsilon_{11}} \right),$$

$$B_{51} = -\frac{1}{r} \frac{\pi}{l} \left( \begin{array}{c} \frac{e_{11}c_{12}e_{11}ac_{31}}{c_{11}\epsilon_{11}c_{11}} - \frac{c_{31}c_{12}}{c_{11}} - \frac{c_{31}e_{11}e_{12}a}{c_{11}\epsilon_{11}} \\ +c_{32} + \frac{e_{13}e_{12}}{\epsilon_{11}}a - \frac{e_{13}c_{12}e_{11}}{\epsilon_{11}c_{11}}a \end{array} \right),$$

$$B_{52} = \left( \frac{\pi}{l} \right)^2 \left( \begin{array}{c} \frac{c_{31}e_{11}e_{11}ac_{13}}{c_{11}\epsilon_{11}c_{11}} - \frac{c_{31}e_{11}e_{13}a}{c_{11}\epsilon_{11}} - \frac{c_{31}c_{13}}{c_{11}} \\ +c_{33} - \frac{e_{13}e_{11}ac_{13}}{\epsilon_{11}c_{11}} + \frac{e_{13}e_{13}}{\epsilon_{11}}a \end{array} \right),$$

$$B_{54} = -\frac{\pi}{l} \left( \frac{c_{31}}{c_{11}} - c_{31} \frac{e_{11}e_{11}a}{c_{11}\epsilon_{11}c_{11}} + \frac{e_{11}ae_{13}}{\epsilon_{11}c_{11}} \right),$$

$$B_{55} = -\frac{1}{r}, \quad B_{56} = -\frac{\pi}{l} \left( \frac{c_{31}e_{11}a}{c_{11}\epsilon_{11}} - \frac{e_{13}}{\epsilon_{11}}a \right),$$

$$B_{61} = -\left( \frac{\pi}{l} \right)^2 e_{15}, \quad B_{63} = -\frac{e_{15}e_{15}}{G} \left( \frac{\pi}{l} \right)^2 - \epsilon_{11} \left( \frac{\pi}{l} \right)^2,$$

$$B_{65} = \frac{e_{15}}{G} \frac{\pi}{l}, \quad B_{66} = -\frac{1}{r},$$

$$d_{11} = \left( \frac{\beta_1}{C_{11}} - \frac{e_{11}ae_{11}\beta_1}{C_{11}\epsilon_{11}C_{11}} - \frac{q_1ae_{11}}{\epsilon_{11}C_{11}} \right),$$

$$d_{13} = \left( q_1 \frac{a}{\epsilon_{11}} + \frac{ae_{11}\beta_1}{\epsilon_{11}C_{11}} \right),$$

$$d_{14} = \frac{1}{r} \left( \begin{array}{c} \frac{C_{21}\beta_1}{C_{11}} - \frac{C_{21}e_{11}ae_{11}\beta_1}{C_{11}\epsilon_{11}C_{11}} - \frac{q_1C_{21}ae_{11}}{\epsilon_{11}C_{11}} \\ +\frac{e_{12}q_1a}{\epsilon_{11}} + \frac{ae_{12}e_{11}\beta_1}{\epsilon_{11}C_{11}} - \beta_2 \end{array} \right),$$

$$d_{15} = -\frac{\partial}{\partial z} \left( \begin{array}{c} -\frac{C_{31}e_{11}ae_{11}\beta_1}{C_{11}\epsilon_{11}C_{11}} + \frac{\beta_1C_{31}}{C_{11}} - \frac{C_{31}q_1ae_{11}}{\epsilon_{11}C_{11}} \\ +\frac{e_{13}q_1a}{\epsilon_{11}} + \frac{e_{13}e_{11}\beta_1a}{\epsilon_{11}C_{11}} - \alpha_3 \end{array} \right),$$

$$f_{11} = \left( \frac{\beta_1}{C_{11}} - \frac{e_{11}ae_{11}\beta_1}{C_{11}\varepsilon_{11}C_{11}} - \frac{q_1ae_{11}}{\varepsilon_{11}C_{11}} \right),$$

$$f_{13} = \left( q_1 \frac{a}{\varepsilon_{11}} + \frac{ae_{11}\beta_1}{\varepsilon_{11}C_{11}} \right),$$

$$f_{14} = \frac{1}{r} \left( \frac{C_{21}\beta_1}{C_{11}} - \frac{C_{21}e_{11}ae_{11}\beta_1}{C_{11}\varepsilon_{11}C_{11}} - \frac{q_1C_{21}ae_{11}}{\varepsilon_{11}C_{11}} \right. \\ \left. + \frac{e_{12}q_1a}{\varepsilon_{11}} + \frac{ae_{12}e_{11}\beta_1}{\varepsilon_{11}C_{11}} - \alpha_2 \right),$$

$$f_{15} = -\frac{\pi}{l} \left( -\frac{C_{31}e_{11}ae_{11}\beta_1}{C_{11}\varepsilon_{11}C_{11}} + \frac{\beta_1C_{31}}{C_{11}} - \frac{C_{31}q_1ae_{11}}{\varepsilon_{11}C_{11}} \right. \\ \left. + \frac{e_{13}q_1a}{\varepsilon_{11}} + \frac{e_{13}e_{11}\beta_1a}{\varepsilon_{11}C_{11}} - \beta_3 \right).$$

### Appendix 3.

Equilibrium equations

$$\frac{d\sigma_r}{dr} + \frac{1}{r}(\sigma_r - \sigma_\theta) = 0, \quad \frac{dD_r}{dr} + \frac{1}{r}D_r = 0. \quad (\text{A1})$$

Strain displacement relations

$$\varepsilon_r = \frac{\partial u}{\partial r}, \quad \varepsilon_\theta = \frac{u}{r}, \quad E_r = -\frac{d\phi}{dr}. \quad (\text{A2})$$

The constitutive equations when specialized to cylindrically orthotropic materials, polarized in the radial direction, may be written as

$$\sigma_r = C_{11}\varepsilon_r + C_{12}\varepsilon_\theta - e_{11}E_r - \beta_1T, \\ \sigma_\theta = C_{12}\varepsilon_r + C_{22}\varepsilon_\theta - e_{12}E_r - \beta_2T, \\ D_r = e_{12}\varepsilon_\theta + e_{11}\varepsilon_r + \varepsilon_{11}E_r + q_1T. \quad (\text{A3})$$

System of simultaneous first-order differential equations

$$\frac{du}{dr} = \sigma_r \left( \frac{1}{C_{11}} - \frac{e_{11}e_{11}}{C_{11}\varepsilon_{11}C_{11}a} \right) \\ - \frac{u}{r} \left( \frac{C_{12}}{C_{11}} + \frac{e_{11}e_{12}}{C_{11}\varepsilon_{11}a} - \frac{e_{11}e_{11}C_{12}}{C_{11}\varepsilon_{11}C_{11}a} \right) \\ + D_r \left( \frac{e_{11}}{C_{11}\varepsilon_{11}a} \right) - T \left( \frac{e_{11}q_1}{aC_{11}\varepsilon_{11}} + \frac{e_{11}\beta_1e_{11}}{C_{11}aC_{11}\varepsilon_{11}} - \frac{\beta_1}{C_{11}} \right),$$

$$\frac{d\phi}{dr} = \frac{-D_r}{\varepsilon_{11}a} + \frac{u}{r} \left( \frac{e_{12}}{\varepsilon_{11}a} - \frac{e_{11}C_{12}}{\varepsilon_{11}C_{11}a} \right)$$

$$+ \sigma_r \frac{e_{11}}{\varepsilon_{11}C_{11}a} + T \left( \frac{q_1}{\varepsilon_{11}} + \frac{\beta_1e_{11}}{C_{11}\varepsilon_{11}} \right),$$

$$\frac{d\sigma_r}{dr} = \frac{\sigma_r}{r} \left\{ \left[ \frac{C_{12}}{C_{11}} - 1 \right] + \left[ e_{12} - \frac{C_{12}e_{11}}{C_{11}} \right] \left[ \frac{e_{11}}{\varepsilon_{11}C_{11}a} \right] \right\}$$

$$+ \frac{u}{r^2} \left\{ \left[ C_{22} - \frac{C_{12}C_{12}}{C_{11}} \right] + \left[ e_{12} - \frac{C_{12}e_{11}}{C_{11}} \right] \right.$$

$$\left. \times \left[ \frac{e_{12}}{\varepsilon_{11}a} - \frac{e_{11}C_{12}}{\varepsilon_{11}C_{11}a} \right] \right\} - \frac{D_r}{r} \frac{1}{\varepsilon_{11}a} \left[ e_{12} - \frac{C_{12}e_{11}}{C_{11}} \right]$$

$$+ \frac{T}{r} \left\{ \left[ \frac{q_1}{a\varepsilon_{11}} + \frac{\beta_1e_{11}}{aC_{11}\varepsilon_{11}} \right] \left[ e_{12} - \frac{e_{11}C_{12}}{C_{11}} \right] - \beta_2 + \frac{\beta_1C_{12}}{C_{11}} \right\},$$

$$\frac{dD_r}{dr} = \frac{-D_r}{r} \quad (\text{A4})$$

where

$$a = 1 + \frac{e_{11}e_{11}}{\varepsilon_{11}C_{11}}.$$

### Nomenclature

$r, \theta, z$	= Cylindrical coordinates
$u, v, w$	= Displacement components
$\sigma_r, \sigma_\theta, \sigma_z$	= Normal stress components parallel to $r$ , $\theta$ and $z$ axis
$\tau_{zr}$	= Shearing stress in cylindrical coordinates
$\varepsilon_r, \varepsilon_\theta, \varepsilon_z$	= Unit elongation (normal strain) components in cylindrical coordinates
$\gamma_{zr}$	= Shearing strain component in cylindrical coordinates
$C_{ij}$	= Material constants for orthotropic materials
$e_{ij}$	= Piezoelectric moduli
$D_m$	= Electric displacement vector
$E_k$	= Electric field
$\varepsilon_{33}$	= Dielectric permittivity constants at constant strain
$r_i$	= Inner radius of the cylinder
$r_0$	= Outer radius of the cylinder
$l$	= Length of the cylinder
$\bar{u}, \bar{w}$	= Nondimensionalized displacement components

$\bar{\sigma}_r, \bar{\sigma}_\theta, \bar{\sigma}_z$	= Nondimensionalized normal stress components parallel to $r, \theta$ and $z$ axis
$\bar{\tau}_{rz}$	= Nondimensionalized shearing stress in cylindrical coordinates
$\bar{r}$	= Nondimensionalized radius
$R$	= Mean radius $(r_0 + r_i)/2$ .

1. Cady, W. G., *Piezoelectricity: An Introduction to the Theory and Applications of Electromechanical Phenomena in Crystals*, McGraw-Hill, New York, 1946.
2. Tiersten, H., *Linear Piezoelectric Plate Vibrations*, Plenum Press, New York, 1969.
3. Kraus, H., *Thin Elastic Shells*, John Wiley, New York, 1967.
4. Kant, T. and Ramesh, C., Numerical integration of linear boundary value problems in solid mechanics by segmentation method. *Int. J. Numer. Methods. Eng.*, 1981, **17**, 1233–1256.
5. Desai, P. and Kant, T., On accurate stress determination in laminated finite length cylinders subjected to thermo elastic load. *Int. J. Mech. Solids*, 2011, **6**(1), 7–26.
6. Heyliger, P. R. and Pan, E., Static fields in magnetoelectroelastic laminates. *AIAA J.*, 2004, **42**(7), 1435–1443.
7. Kapuria, S., Sengupta, S. and Dumir, P. C., Three-dimensional solution for a hybrid cylindrical shell under axisymmetric thermoelectric load. *Arch. Appl. Mech.*, 1997, **67**, 320–330.
8. Heyliger, P. R., A note on the static behaviour of simply supported laminated piezoelectric cylinders. *Int. J. Solids Struct.*, 1997, **34**(29), 3781–3794.
9. Galic, D. and Horgan, C. O., Internally pressurized radially polarized piezoelectric cylinders. *J. Elast.*, 2002, **66**, 257–272.
10. Rajapakse, R. K. N. D., Chen, Y. and Senjuntichai, T., Electro-elastic field of a piezoelectric annular finite cylinder. *Int. J. Solids Struct.*, 2005, **42**, 3487–3508.
11. Ding, H. J., Guo, F. L., Hou, P. F. and Zou, D. Q., On the equilibrium of piezoelectric bodies of revolution. *Int. J. Solids Struct.*, 2000, **37**, 1293–1326.
12. Wang, X. and Zhong, Z., A finitely long circular cylindrical shell of piezoelectric/piezomagnetic composite under pressuring and temperature change. *Int. J. Eng. Sci.*, 2003, **41**, 2429–2445.
13. Lim, C. W. and Lau, C. W. H., A new two-dimensional model for electro-mechanical response of thick laminated piezoelectric actuator. *Int. J. Solids Struct.*, 2005, **42**, 5589–5611.
14. Wu, C.-P. and Tsai, T.-C., Exact solutions of functionally graded piezoelectric material sandwich cylinders by a modified Pagano method. *Appl. Math. Model.*, 2011; doi: 10.1016/j.apm.2011.07.077.
15. Ying, Z. G., Wang, Y., Ni, Y. Q. and Ko, J. M., Stochastic response analysis of piezoelectric axisymmetric hollow cylinders. *J. Sound Vib.*, 2009, **321**, 735–761.
16. Larbi, W. and Deu, J.-F., A 3D state-space solution for free-vibration analysis of a radially polarized laminated piezoelectric cylinder filled with fluid. *J. Sound Vib.*, 2011, **330**, 162–181.
17. Saviz, M. R. and Mohammadpourfard, M., Dynamic analysis of a laminated cylindrical shell with piezoelectric layers under dynamic loads. *Finite Elem. Anal. Des.*, 2010, **46**, 770–781.
18. Li, X.-F., Peng, X.-L. and Lee, K. Y., Radially polarized functionally graded piezoelectric hollow cylinders as sensors and actuators. *Eur. J. Mech. A/Solids*, 2010, **29**, 704–713.
19. Khdeir, A. A. and Aldraihem, O. J., Exact analysis for static response of cross ply laminated smart shells. *Comput. Struct.*, 2011, doi:10.1016/j.compstruct.2011.07.013.
20. Timoshenko, S. and Goodier, J., *Theory of Elasticity*, McGraw-Hill, New York, 1951.
21. Gill, S., A process for the step-by-step integration of differential equations in an automatic digital computing machine. *Proc. Cambridge Philos. Soc.*, 1951, **47**(1), 96–108.

Received 13 March 2011; revised accepted 29 November 2011